International Journal of Pharmaceutics 371 (2009) 47–55

Contents lists available at ScienceDirect

International Journal of Pharmaceutics

journal homepage: www.elsevier.com/locate/ijpharm

Voltammetric sensor for barbituric acid based on a sol–gel derivated molecularly imprinted polymer brush grafted to graphite electrode

Amit Kumar Patel, Piyush Sindhu Sharma, Bhim Bali Prasad*

Analytical Division, Department of Chemistry, Banaras Hindu University, Varanasi 221005, India

ARTICLE INFO

Article history:
Received 22 October 2008
Received in revised form 11 December 2008
Accepted 11 December 2008
Available online 24 December 2008

Keywords:
Barbituric acid sensor
Molecularly imprinted polymer
Sol–gel
Graphite electrode
Differential pulse
Cathodic stripping voltammetry

ABSTRACT

A voltammetric sensor based on a molecularly imprinted polymer (MIP) brush grafted to sol–gel film on graphite electrode is reported for the selective and sensitive analysis of barbituric acid (BA) in aqueous, blood plasma, and urine samples. The modified electrode was preanodised at +1.6 V (vs. saturated calomel electrode), where encapsulated BA involved hydrophobically induced hydrogen bondings, in MIP cavities exposed at the film/solution interface, at pH 7.0. Scanning electron microscopy (SEM) was employed to characterise the surface morphology of the resultant imprinted film of MIP brush. The differential pulse, cathodic stripping voltammetry (DPCSV) technique was employed to investigate the binding performance of the sol–gel-modified imprinted polymer brush, which yielded a linear response in the range of 4.95–100.00 $\mu g\,mL^{-1}$ of BA with a detection limit of 1.6 $\mu g\,mL^{-1}$ ($S/N = 3$).

1. Introduction

The modification and the control of surface properties using tailored macromolecular architectures are essential for the fabrication of chemical sensors. Such architectures include covalently anchored polymer brushes which are generally prepared using mainly two strategies, i.e., "grafting-to" and "grafting-from" (Advincula et al., 2004; Pyun and Matyajaszewski, 2001). Whereas the "grafting-from" technique is a widely used approach to obtain polymer brushes with high grafting densities, a rigorous characterisation of the brushes after grafting is necessarily required to comprehand the morphology of polymer brushes grown in the bulk. On the other hand, "grafting-to" approach is apparently advantageous of having the well-characterised linear brush structure. Several tethering methods are known in the literature to graft polymer brushes on silicon substrate, e.g., esterification, condensation, or amidation reactions between ω-functionalised polymer and silanols covering silicon wafers or functionalised self assembly monolayers (SAMs) (Zdyrko et al., 2006; Walters and Hirt, 2007; Julthongpiput et al., 2003). In all these cases, the polymer adsorption which reduces grafting density of resulting brushes was found problematic. This was, however, successively passivated using a vinyl-functionalised SAM and by taking advantage of the grafting of SiH-terminated polymers using Pt-catalysed hydrosylation (Casoli et al., 2001; Marzolin et al., 2001).

In the present work, we adapted a simple "grafting-to" procedure by tethering a MIP over a sol–gel-modified graphite surface. The immobilisation of MIP was carried out after 'syneresis' (a stage between ageing and drying) (Podbielska and Ulatowska-Jarza, 2005) of sol–gel. This was found to be advantageous to expose microcativities of MIP outwardly at the surface for unhindered analyte rebinding, shrouding residual silanols (which promote non-specific binding), and for passivating the surface toward any adsorption of brush precursors.

The model test analyte (template) selected in the present work for analysis was BA, a core molecule, which belongs to the most vulnerable family of medicinal agents used as known sedative hypnagouge. The BA and its derivatives are also ascribed as poisonous and irritating toxicants after frequent abuse either alone or in combination with alcohol. Barbiturates overdose is manifested by the oversuppression of the CNS. The manifestations of CNS suppression are dose dependent. In mild overdose, lethargy, slurred speech, nystagmus and ataxia are common. In severe acute overdose, CNS and respiratory depression may progress to Cheyne-Stokes respiration, areflexia, oliguria, tachycardia, hypotension, hypothermia and deep coma with slight constriction of the pupils. The blood pressure will drop secondary to the direct effect of the drug and hypoxia of the medullary vasomotor centre leading to arteriolar dilution, depression of cardiac contractility and vasomotor smooth muscle. Death may occur as a result of typical shock syndrome indicated by the apnea, circulatory collapse and

* Corresponding author. Tel.: +91 9451954449.
E-mail address: prof.bbpd@yahoo.com (B.B. Prasad).

0378-5173/$ – see front matter © 2008 Elsevier B.V. All rights reserved.
doi:10.1016/j.ijpharm.2008.12.016

respiratory arrest. EEG examination may show a "flat" tracing indicating the cessation of the electrical discharge from the brain. Acute overdose of intravenous (IV) barbiturate especially if administered too rapidly may lead to severe respiratory depression, apnea, laryngospasm, bronchospasm and hypertension. These symptoms are reversible with the discontinuation or reduction of the rate of IV administration. Barbiturates may also cause necrosis of the sweat gland and bullous cutaneous lesion which is not related to hypersensitivity reaction. The diagnosis of barbiturate poisoning is done based on the presence of the above manifestations confirmed by the elevated blood levels of barbiturate. The blood levels of barbiturate may not necessarily correlate well with the outcome of the therapy especially in those patients who consume barbiturate together with other CNS drugs. The potential fatal level of barbiturates is 10 $\mu g\,mL^{-1}$ with the intermediated and short-acting barbiturates (Blanke, 1986) and greater than 200 $\mu g\,mL^{-1}$ with the long-acting barbiturates (Bailey and Jatlow, 1975). The barbiturate concentrations greater than 200 $\mu g\,mL^{-1}$ in a living patient should warrant serious consideration of BA ingestion.

The dilution of sample with limited volume of blood plasma (e.g., in newborns or if blood is taken by capillary) is essentially required to mitigate the matrix complications, if preliminary treatment (i.e., deproteinisation/ultrafiltration, etc.) of the sample, which oftenly causes inaccuracies in results, is to be avoided in the case of a small content of the blood plasma sample. Under such condition, microanalysis of barbiturates in diluted body fluids, with a narrow therapeutic concentration index and variable rates of elimination, requires a sensitive method development for biomedical (clinical) applications. Different methods such as chromatography (Ubbink et al., 1993; Aboul-Enein et al., 1996; Garcia-Borregon et al., 2000), mass spectrometry (Van Langenhov et al., 1982), capillary electrophoresis (You et al., 2000), infrared spectrophotometry (Pawelczyk et al., 1972), coulometry (Nematollahi and Hesari, 2001), spectrophotometry (Medien, 1996; Aman et al., 1997; Medien and Zahran, 2001; Nagaraja et al., 2001), polarography (Romer et al., 1977), colorimetry (Bartzatt, 2002) and sensors (Prasad and Lakshmi, 2005) have been reported for the determination of BA. Some of these methods are time consuming and suffer from the lack of selectivity and/or short linear dynamic range, having higher limit of detection, and reagents used are not commercially available. Till date, no MIP for BA is reported barring our earlier work of BA sensor based on MIP-modified hanging mercury drop electrode (HMDE) (Prasad and Lakshmi, 2005). The actual limitation is on-line or in-field detection of BA, which appeared not to be feasible with MIP-modified HMDE sensor. This inculcated a genuine surge upon the development of a solid electrode sensor, which could serve as a potential device for in-field studies and at the same time could be cost-effective and disposable, for sensitive and selective detection of BA in real samples.

2. Experimental

2.1. Instruments and chemicals

All the electrochemical experiments were carried out with a model 264A Polarographic Analyser/Stripping voltammometer, using a single compartment three electrode cell, in conjunction with a X-Y recorder (PAR Model RE 0089). A platinum wire served as auxiliary electrode, a saturated calomel electrode (SCE) was the reference electrode, and the MIP-modified sol–gel film graphite electrode was used as a working electrode. All potential examined and reported are with respect to SCE. The morphological evaluation of MIP-coated graphite electrode was made by scanning electron microscope (SEM, Model-XL20 Philips, The Netherlands). Infrared spectra of coating material were recorded by FT-IR spectrometer (Jasco, FT/IR 5300). A laser surface profilometer (Perthometer, PGK 120, Mahr, Germany) was used to measure the film thickness and roughness-profile of the coating layer.

Spectroscopic grade graphite rod (3.5 mm diameter) was used for the modification. Reagents melamine (mel), chloranil (chl), tetraethoxysilane (TEOS), and BA were purchased from Loba Chemie India, Otto, Chemie, India, SD Fine, India, and Fluka, Germany. Other chemicals and interferents used in the present investigation were of analytical grade. The solvents, dimethylformamide (DMF) and ethanol, were of HPLC quality. Graphite powder (1–2 μm) was analytical reagent grade sample and used as received. Triple distilled water was used throughout for the preparation and dilution; the pH values of test samples were maintained using aqueous solution of sodium hydroxide. The real test samples (human blood plasma and urine) were obtained from a local patholab.

2.2. MIP-coated sol–gel preparation

The MIP [poly (mel-co-chl)] and respective non-imprinted polymer (NIP) were prepared and characterised according to the procedure described earlier (Prasad and Lakshmi, 2005). In brief, a reaction mixture of equimolar DMF solutions of mel and chl was first heated at ca 160 °C for an hour and then mixed with an equimolar DMF solution of BA and refluxed for 4 h with intermittent shaking (notably, there was no effect of DMF solution on BA for a longer period at ca 160 °C). The solvent DMF was almost evaporated at ca 160 °C followed by ethanol washing to remove unreacted residual monomers if any, from the resulting slurry. The NIP was prepared following the similar procedure but in the absence of template. An optimised amount of MIP slurry (0.3 mL, 12×10^3 $\mu g/mL$ in DMF) was mixed with 1.0 mL sol–gel slurry (1.0 mL TEOS, 1.0 mL ethanol, 0.5 mL H_2O, and 50 μL 0.1 M HCl) at 'syneresis' stage obtained by the mechanical stirring at 600 rpm for ~80 min. The graphite powder (1–2 μm, 50 mg) was also mixed during mechanical stirring to obtain a semi-solid viscous liquid of MIP adduct-sol–gel composite. Similar procedure was followed to obtain NIP-coated sol–gel, but in the absence of template.

2.3. Electrode preparation and voltammetric procedure

Graphite rod electrodes (6 mm long) were first coated with an epoxy spray to insulate the rods, and then each one was inserted into a glass sleeve; the protruding end of the graphite (1.5 mm) was exposed by polishing on emery papers (No. 100, 400) while the opposite end was made available for the electrical contact with the help of a copper wire through the glass tube. The polished end of each graphite rod was coated with one drop (20 μL) of MIP adduct–sol–gel viscous solution at the spin rate of 2600 rpm for 90 s and dried in a desiccator for ~24 h. For the complete extraction of BA template from the MIP film, hot water (~75 °C) was used (two extractions, equilibration time 10 s, 5 mL portions) until no DPCSV peak corresponding to trace BA was obtained. During solidification of the film and template removal steps, chloride ions from MIP network were also washed away but its cavity conformation remained intact and stable (Lakshmi et al., 2006). All the MIP- and NIP–sol–gel electrodes were left to dry under room conditions. These electrodes were preconditioned by soaking in water for atleast 1 h before use.

The cell container containing 10 mL aqueous solution (pH 7.0) of BA (in absence of any supporting electrolyte) was brought under the modified electrode for an optimised accumulation time 90 s at +1.6 V (vs. SEC) and both cyclic voltammetry (CV) and DPCSV runs were recorded under cathodic stripping mode from +0.6 V and +0.5 V and terminated at −0.1 and −0.3 V, respectively (scan rate 10 mVs^{-1}, pulse amplitude 25 mV, equilibration time 15 s, temperature 25 ± 1 °C). The method of standard addition was followed for the quantification of DPCSV peaks.

The electrode regeneration in the present instance was easier simply using hot water washings (2 × 5 mL, equilibration time 10 s for each washing); no DPCSV peaks of BA was observed in the third washing.

3. Results and discussion

3.1. Characterisation of sol–gel-immobilised MIP

Structural characterisations of sol–gel, sol–gel–MIP adduct and sol–gel–MIP using FTIR were same as those described in an earlier work (Patel et al., 2008) because polymer networks were structurally identical. The multiple hydrogen bonding interactions in aqueous environment between MIP and BA have already been established as 'hydrophobically driven hydrogen bondings' (Fig. 1) (Prasad and Lakshmi, 2005).

Insofar as the surface morphology of MIP coating is concerned, the SEM image (Fig. 2a) of MIP adduct immobilised onto sol–gel-modified surface, under the magnification of 7398×, revealed a dense film layer amidst carbon representing a clear visualisation of MIP brush semi-pattern (overlapped) on the electrode surface. The total average thickness (h) all along the coated surface was measured for every batch of the prepared electrodes (10 electrodes per batch) as 19.07 ± 1.69 μm. This measurement is based on the film "grafted-to" graphite rod obtained by cutting its protruded surface as a disc. The straight tethering of the polymer chain did not occur in the present instance because of massive overlapping of polymer brush, notwithstanding the fact that the brush height (19.07 μm) is significantly higher than the end-to-end distance ($\langle r^2 \rangle^{1/2}$ = 0.011 μm) of the polymer chain. The reason being an assumption of a hydrophobically collapsed state (MIP and BA are hydrophobic in nature) while grafting in DMF medium. Interestingly, after the template removal from the MIP-BA adduct in the film, the MIP brush still maintained the hydrophobically collapsed status but with a high degree of porosity (Fig. 2b). The force minimum for collapse arises from attractive polymer segment

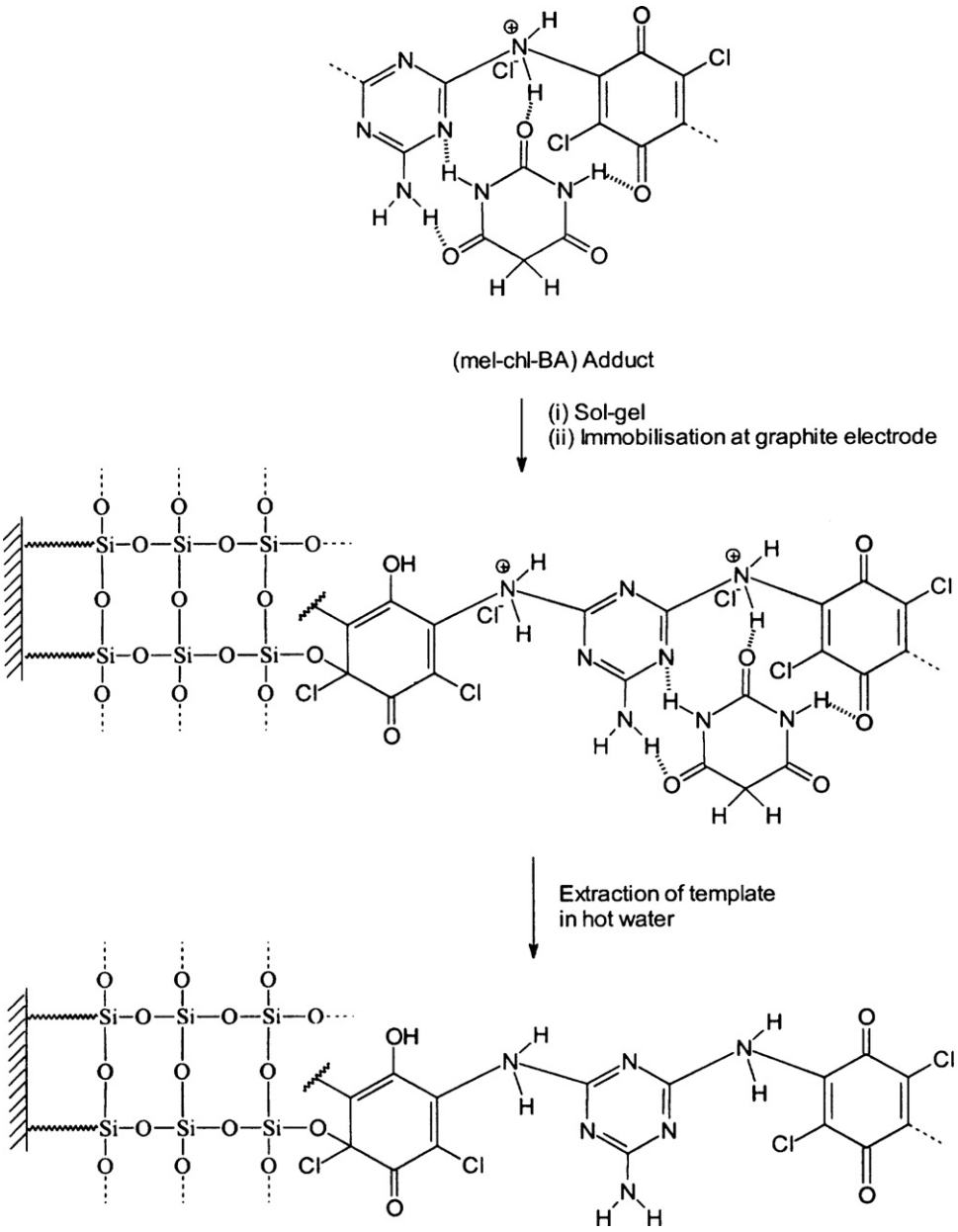

Fig. 1. Schematic representation of the preparation of MIP–sol–gel-modified graphite electrode.

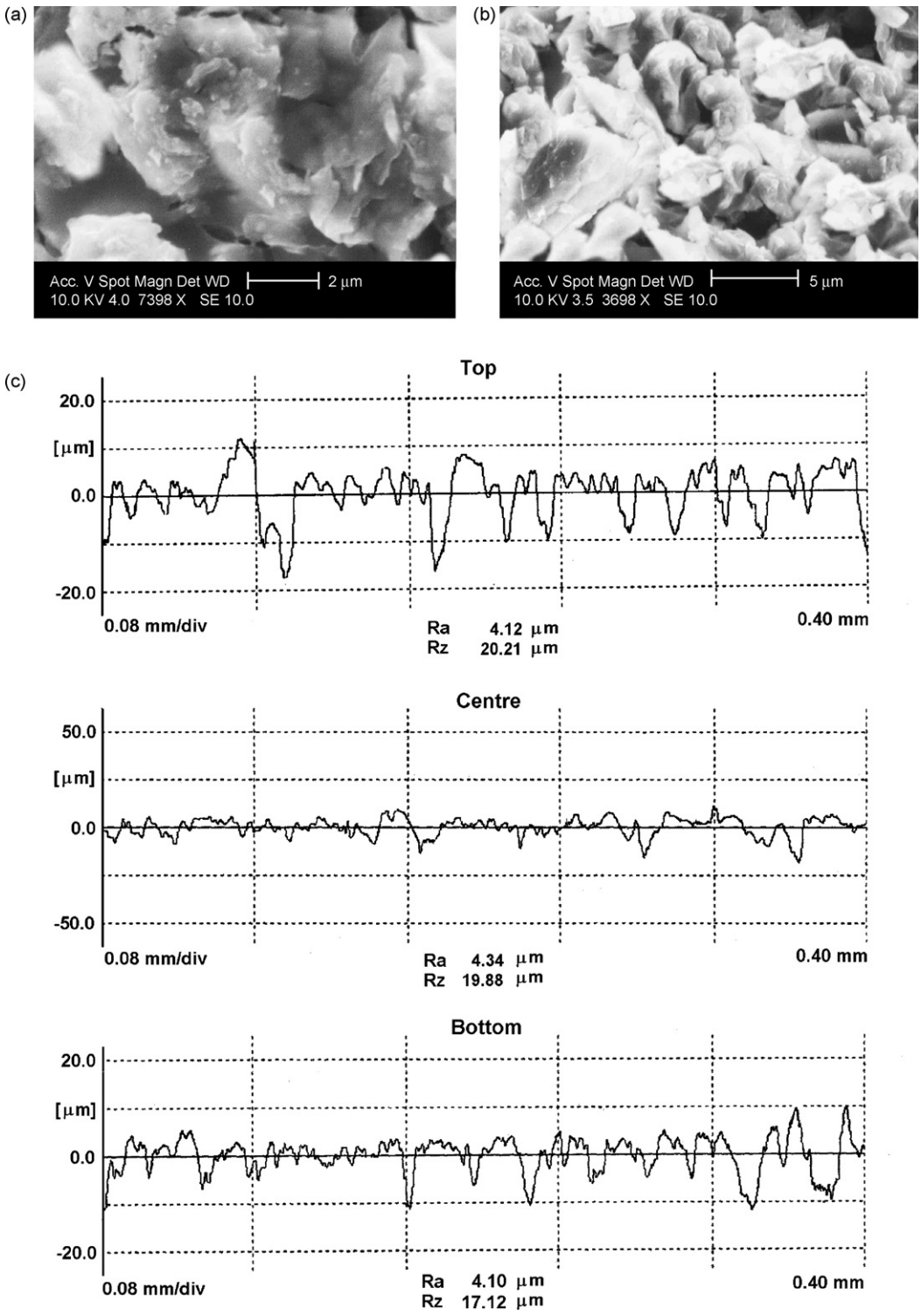

Fig. 2. (a) SEM image of sol–gel–MIP–BA adduct composite on graphite electrode at 7398X, (b) SEM image of sol–gel–MIP composite on graphite electrode at 3698X in absence of template, and (c) roughness profile of MIP–BA adduct on sol–gel-modified graphite surface within sampling length at top, centre and bottom.

interactions (mel-chl BA adduct, Fig. 1), whose number increases with increasing compression of the brush surfaces until, with further compression the restriction in conformational degree of freedom finally dominates and gives rise to strong, steric repulsion. The roughness profiles of a cross-section of immobilised MIP-BA adduct onto sol–gel-modified graphite electrode (*z*-axis in μm) are shown in Fig. 2c, where Ra is the arithmetic average of absolute value of the roughness profile ordinate and Rz is arithmetic mean of vertical distances between highest peak and deepest valleys within a sampling length at top, centre and bottom.

The grafting process in the present case led a chemically homogeneous MIP fully covering the sol–gel surface as evident from SEM images (Fig. 2a and b). The nanometer-scale morphology observed

here most probably results from the heterogeneity of the brush layer in the terms of grafting density ($\sigma = 5.4$ chains/nm^2) as calculated using relation (1)

$$\sigma = \frac{h\rho \mathrm{Na}}{\mathrm{Mn}} \quad (1)$$

where h is the thickness of the dry polymer brushes, Na is Avogadro's number, Mn (5098.81 g mol^{-1}) is the MIP-BA adduct number average molecular weight, and ρ (2.47×10^3 g/m^3) is the density of the anchored polymer. The average distance between grafting point ($D = 2(\pi\sigma)^{-1/2} = 0.48$ nm) is lower than the end-to-end distance of the polymer (11.6 nm), confirming that the MIP grafted layer is in the brush regime (Luzinov et al., 2000; De Gennes, 1980; Zhulina et al., 1990; Netz and Schick, 1998). However, the grafting density (5.4 chains/nm^2) of polymer brushes is significantly higher than the maximum grafting density (ν_{max}) achievable via a "grafting-to" approach. As per Auroy et al. (1991), the grafting density of polymer brush is generally governed by the brush polymerisation degree (N) and the polymer weight fraction in the grafting solution (ϕ), as given by the relation (2)

$$\nu \sim \frac{N^{-1/2}\phi^{7/8}}{\alpha^2} \quad (2)$$

where α represents the segmental length of monomer ($\alpha \sim 1.16$ nm for MIP). Thus, for MIP brush formed for a weight fraction of 100 wt% (i.e., $\phi = 1$), $\nu_{max} = 0.23$ chains/nm^2. However, the experimental grafting density (5.4 chains/nm^2) in the present instance appeared to be of a collapse state of an optimised highly dense brush pattern on sol–gel surface, in the DMF medium of coating solution.

3.2. Sensor development

An interpenetrating network (IPN) (Fig. 1) of graphite–sol–gel–MIP hybrid material produced under two-steps coating protocol resulted in two microphases. The first microphase between graphite and sol–gel occurred via physical sorption, while the second microphase involved covalently bonded tethering of MIP molecules as polymer brushes. The sol–gel must be homogeneous and crack-free at syneresis stage so that polymer brushes may protrude outwardly to recapture template, without any steric hindrance, at the film/solution interface. Almost every silanol groups were used up in polymer tetherings and residual silanols, if any, which contribute non-specific bindings, were actually covered by MIP film layer. In the present investigation, we have concentrated on tethering polymer brush particularly on the sol–gel for several reasons. The sol–gel/graphite surface is stronger owing to in-depth coating in graphite pores, than sol–gel/gold interface. However, the film usually flakes off the Au-electrode surface (Zhang et al., 2006). The second interface involved a caged Si–OC bond structure (Xu et al., 2004) where the Si–O bond dissociation energy is 96–133 kcal mol^{-1} (Dyer, 2003; Walsh and Becerra, 1998). Sol–gel and graphite substrate are low in cost, stable, smooth, and easy to prepare, whereas gold films are prone to delamination, or some times rough, and require more effort to prepare and handle (Love et al., 2002). A pool of electrostatic interactions between electron-rich chl-mel functionalities of MIP and positively charged +1.6 V (vs. SCE) graphite surface rendered additional stability to IPN hybrid. The incorporation of carbon powder as much as 50 mg in the initial mixture of sol–gel and MIP-adduct solution enabled a higher film conductivity and less shrinkage; any amount higher than this caused a restriction in the film permeability and thereby decreased DPCSV response.

3.3. Voltammetric behaviour

In the present work, the use of any supporting electrolyte was avoided so as to remove unnecessary complication of anionic oxidation at positively charged electrode. As a matter of fact, in stripping voltammetry ions consumed or produced during electrode process are actually transported across the polymer film rather than the bulk solution (Kaaret and Evans, 1988). Furthermore, the dissolved oxygen of the cell content is consumed in the generation of electron-transfer mediating groups such as —C=O and —C—OH on the graphite surface at the preanodised condition, and therefore, deaeration was not required. At +1.6 V (vs. SCE), the entrapped BA molecules in MIP cavities were instantly reoxidised as BA radicals and then stripped off from progressively increasing negatively charged electrode surface under electrostatic repulsion (Prasad and Lakshmi, 2005). However, both cathodic and anodic stripping CV peaks (Fig. 3 inset) were found to be broader in shape reflecting a sluggish quasi-reversible electron-transfer behaviour. This could be attributed to the difficult stripping as a consequence of strong sorption of BA, into intra-molecular polymer brush cavities, transported through the channelised pores. The charge transports from

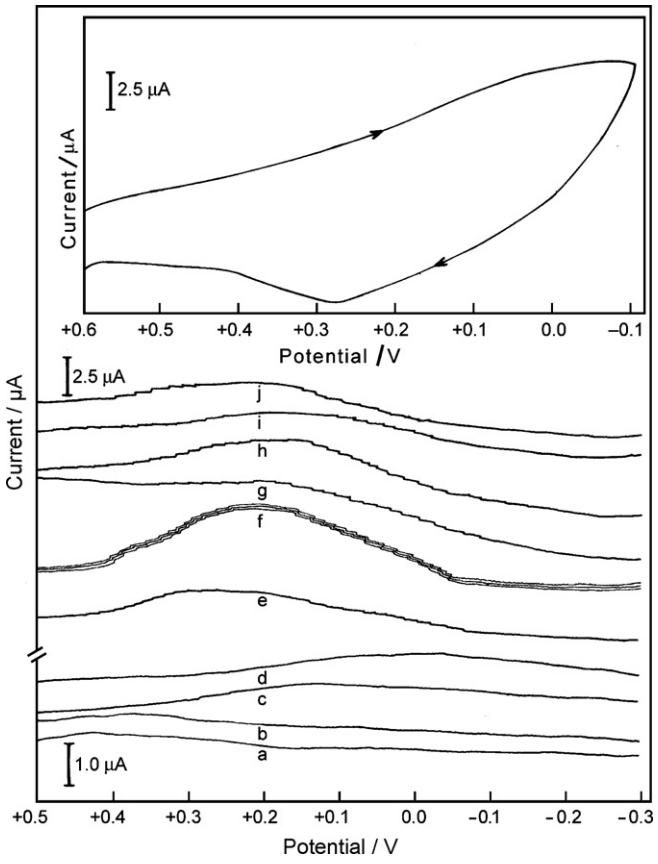

Fig. 3. DPCSV runs of BA (concentration 45.45 μg mL^{-1}) with (a) sol–gel-modified graphite elctrode; (b) MIP-modified graphite electrode; (c) BA imprinted sol–gel-modified graphite electrode; (d) NIP–sol–gel-modified graphite electrode; and (e) MIP–sol–gel-modified graphite electrode. Multiple DPCSV runs of BA [concentration 83.33 μg mL^{-1} in the presence of mixture of interferents (UA, Tph, Ura, phBA, Cre, TBA, Caff; 50.00 μg mL^{-1} each)] with (f) MIP–sol–gel-modified graphite electrode. DPCSV of BA (concentration 23.80 μg mL^{-1}) in human blood plasma with (g) NIP–sol–gel-modified graphite electrode and (h) MIP–sol–gel-modified graphite electrode. DPCSV of BA (concentration 37.03 μg mL^{-1}) in human urine with (i) NIP–sol–gel-modified graphite electrode and (j) MIP–sol–gel-modified graphite electrode. Inset figure shows a typical cyclic voltammogram of BA (28.30 μg mL^{-1}) aqueous solution in stripping mode with MIP–sol–gel-modified graphite electrode. Other operational conditions for all DPCSV runs were: preanodisation potential +1.6 V (vs. SCE), preanodisation time 90 s, pH 7.0, scan rate 10.0 mV s^{-1}.

Table 1
Analytical results of DPCSV measurements of BA in different samples at MIP–sol–gel-modified graphite electrode.

Sample	Analyte BA concentration ($\mu g\ mL^{-1}$)	Determined value[a] (mean ± S.D.) ($\mu g\ mL^{-1}$) with MIP—sol-gel modified graphite electrode	Recovery[b] (%)	*RSD*[c] (%) (n =3)	Correlation coefficient	IF[d]	t^e
Distilled water	4.95	4.86 ± 0.01	98.2	0.2			
	14.56	15.85 ± 0.63	108.8	4.0	1.00		
	45.45	45.26 ± 0.75	99.6	1.6		3.4	
	83.33	82.78 ± 0.51	99.3 [95(i), 90(ii), 80 (iii), 75 (iv)]	0.6		3.1	
Diluted human urine (spiked)	9.80	9.71 ± 0.48	99.0	4.9			
	37.03	36.58 ± 0.96	98.8	2.6	1.00	1.9	
	53.57	53.01 ± 0.54	98.9	1.0		1.4	
Diluted human blood plasma (spiked)[f]	4.95	4.95 ± 0.26 (4.12 ± 0.01)	100.0	5.2			t_{cal} = 2.01
	12.19	12.92 ± 1.11 (12.88 ± 0.01)	105.9	8.5	1.00		t_{tab} =4.30
	23.80	24.35 ± 1.55 (23.84 ± 0.06)	102.3	6.4		1.2	

[a]Average of three replicate determinations (S/N = 3) with MIP–sol-gel modified graphite electrode.
[b]Amount of analyte determined/ amount of analyte taken; values in parenthesis indicate recoveries after (i) 18, (ii) 19, (iii) 20, (iv) 21 consecutive runs recorded by same electrode regenerated at every alternate day.
[c]Relative standard deviation.
[d]Imprinting factor.
[e]Student's t-test for comparison of two methods at confidence level of 95%.
[f]Values in parentheses indicate concentration ($\mu g\ mL^{-1}$) determined by the standard MIP–sensor method (Prasad and Lakshmi, 2005).

bulk to the film (homogeneous electron-transfer) and from film to the electrode surface (heterogeneous electron-transfer) might occur via electron-hopping mechanism, which appeared to be sluggish across both microphases amidst carbon powder dispersion in the present case. Because of the broadness of the CV peaks, quantification was apparently difficult. However, DPCSV peaks (Fig. 3f) with sol–gel-modified graphite electrode are symmetrical within the pulse amplitude of 25 mV and hence easily quantifiable. For a comparative study, we have also prepared the different kind of graphite modified electrodes using various coatings, viz., sol–gel, MIP, BA imprinted sol–gel (BA dopant in sol–gel), NIP–sol–gel and MIP–sol–gel, all with embedded carbon powder. The first two electrodes (sol–gel and MIP) were found to be non-responsive (Fig. 3a and b), whereas BA template sol–gel-modified graphite electrode (Fig. 3c) was active to respond BA ($\geq$9.80 $\mu g\ mL^{-1}$). The last three sol–gel-modified electrodes with surface attached NIP/MIP where found responsive for BA detection in aqueous (Fig. 3d–f), human blood plasma (Fig. 3g and h), and in urine (Fig. 3i and j) sample. Unfortunately, non-specific contributions to the DPSCV current prevailed in aqueous solution ($\geq$28.3 $\mu g\ mL^{-1}$) and in real samples (at any concentration level of BA) with NIP–sol–gel-modified graphite electrode (Fig. 3d, g, i) despite protein-resistance characteristic of polymer brush. However, such problem was successfully resolved via multiple water-washings of both NIP and MIP–sol–gel-modified graphite electrodes after BA recapture from the test solutions. This process enabled specific hydrophobic bound BA to be retained in the MIP cavity while other interferents and non-specific BA molecules were easily washed away with water. The observed DPCSV current with MIP–sol–gel-modified graphite electrode was found to be reproducible after regeneration of the same electrode, even in the presence of a mixture of various interferents, as is evident from the multiple runs shown in Fig. 3f. Insofar as electrode to electrode variation is concerned, all measurements revealed a high degree of precision (*RSD* 0.6%, n = 3) with quantitative recovery (83.33 $\mu g\ mL^{-1}$, Table 1) attainable with each electrode in the present instance. A single electrode could be used for as many as 17 consecutive experiments with quantitative (100%) recoveries (Table 1). The quantitative (100%) recoveries of BA (Table 1) in dilute biological samples indicate that any minor protein-fouling on the polymer brush (if any, even after dilution) is not effective.

3.4. Optimisation of analytical parameters

For modification of graphite electrode the optimisation of spin rate and spin time is necessary to obtain a crack-free monolayer coating. In the present work, a spin rate of 2600 rpm and a spin time of 90 s were found to be the most appropriate parameters to respond maximum DPCSV response. The spin rate and spin time lesser or higher than the above parameters always revealed a drop in DPCSV response. Similar is the situation for the accumulation time of the analyte which revealed an optimised time of 90 s identical to that for sol–gel–MIP film coating. There are poor partitioning of analyte across film/solution interface and poor stability of the MIP–BA adduct, respectively, for lower and higher times given for the deposition of either of film and analyte. The poor hydrogen bonding basicity of the polymer at higher concentration and restricted diffusion-coefficient of analyte across the dense film of MIP brush in aqueous environment might be considered crucial under blocking effect of the binding sites in MIP for BA entrapment. This could be the reason for a drastic fall in the current response at higher polymer concentration ($\geq 12 \times 10^3$ $\mu g\ mL^{-1}$). The electrode catalytic action with optimised polymer amount in monolayer film is effective, where electrogenerated mediators may form stable carbon–carbon bond with active methylene group of BA at +1.6 V

(vs. SCE), realising a faster response time of 90 s towards forming a stable guest–host complex by hydrophobically driven multiple hydrogen bondings in aqueous environment. Any potential lesser or higher than +1.6 V (vs. SCE) revealed a decrease in DPCSV response presumably because of insufficient electrocatalytic action, resulting in incomplete BA oxidation, and film unstability as well as difficult cathodic stripping of template. The optimum DPCSV response of BA rebinding in neutral solution was because of electrostatic attraction of BA (anionic at pH 7.0) with positively charged modified electrode, besides the prevalent hydrophobicity to promote multiple hydrogen bonds. The imprinting factors (i.e., the ratio of current response of MIP to the current response of NIP) realised by MIP- and NIP-modified sol–gel electrodes (without water-washings) in real samples are approximately half to that of BA solution in distilled water (Table 1) (conc. $\geq$28.3 $\mu g\,mL^{-1}$) and this reflected a higher magnitude of non-specific bindings in the complex matrices of real samples. Since the amount of analyte adsorbed under non-specific bindings is normally equal on both MIP and NIP, it is recommended that both types of modified electrode be properly washed with water so as to remove the non-specific residues from the electrode surface. Fortuitously, in the present instance, nearly one washing (1×5.0 mL) with water was found sufficient to eliminate any DPCSV current responded by NIP–sol–gel-modified electrode. Furthermore in real sample, any preliminary treatment was deliberately avoided to restrain from errors in trace analysis; instead, the dilution of biological fluids blood plasma (100-fold) and urine (100-fold) actually helped to save the electrode from fouling and non-specific sorption as well, by equally diluting both interferents and complex matrices. The reproducibility of BA in dilute blood plasma (Table 1) was not as good as the one obtained in urine or in water; however, the recovery was good. This may be attributed to the fact that the protein-fouling effect on the polymer brush still prevailed to some extent, despite the dilution of blood plasma sample. Nevertheless, it is clinically suitable to only dilute the samples, provided the selectivity and sensitivity of the proposed method, as evident from the quantitative (100%) recoveries in the present instance (Table 1), are quite sufficient for the detection of traces of the analyte in highly diluted biological samples, in which the concentrations of interfering species are diluted to negligible concentrations and the problem of matrix interference could maximally be solved simply by dilution.

The DPCSV response of BA for the test sample was found to increase continuously with the increase in concentration, indicating binding isotherm perfectly linear for all the samples studied. The limit of detection (LOD) is calculated on the basis of distinguishable signal S_m and the slope m of linear regression for entire range of concentration of analyte using following equation (Skoog et al., 1998)

$$\mathrm{LOD} = \frac{S_m - \bar{S}_{bl}}{m}$$

where S_m is equivalent to the sum of mean blank signal $\bar{S}_{bl}$ plus a multiple three of the standard deviation of the blank (S_{bl}). The following calibration equations were obtained for the aqueous, blood plasma, and urine samples, with their respective LODs:

- Aqueous medium (concentration range 4.95–100.00 $\mu g\,mL^{-1}$) $I_{PC} = (0.0300 \pm 0.0007)c + (0.04 \pm 0.02)$ $\nu = 1.00$, $n = 8$, LOD = 1.6 $\mu g\,mL^{-1}$ (3σ, RSD = 1.25%).
- Blood plasma sample (concentration range 4.95–55.55 $\mu g\,mL^{-1}$): $I_{PC} = (0.0600 \pm 0.0001)c + (0.12 \pm 0.05)$ $\nu = 1.00$, $n = 7$, LOD = 1.8 $\mu g\,mL^{-1}$ (3σ, RSD = 1.00%).
- Urine sample (concentration range 9.80–72.64 $\mu g\,mL^{-1}$): $I_{PC} = (0.0500 \pm 0.0001)c + (0.08 \pm 0.05)$ $\nu = 1.00$, $n = 5$, LOD = 3.4 $\mu g\,mL^{-1}$ (3σ, RSD = 1.76%).

where I_{PC} is the DPCSV peak current in μA and c is the concentration of BA in $\mu g\,mL^{-1}$. The present method is also compared with the results obtained by a voltammetric method (Prasad and Lakshmi, 2005) for human blood plasma sample (Table 1). Although both methods have similar order of precision within the concentration range studied [student t-test: $t_{cal} < t_{tab}$, confidence level 95%, $\nu = 1.00$], the proposed sensor is portable, disposable, and apparently most suitable for in-field sensing of BA, despite being inferior in terms of the sensitivity vis-a-vis MIP – modified HMDE sensor (LOD = 0.54 $\mu g\,mL^{-1}$).

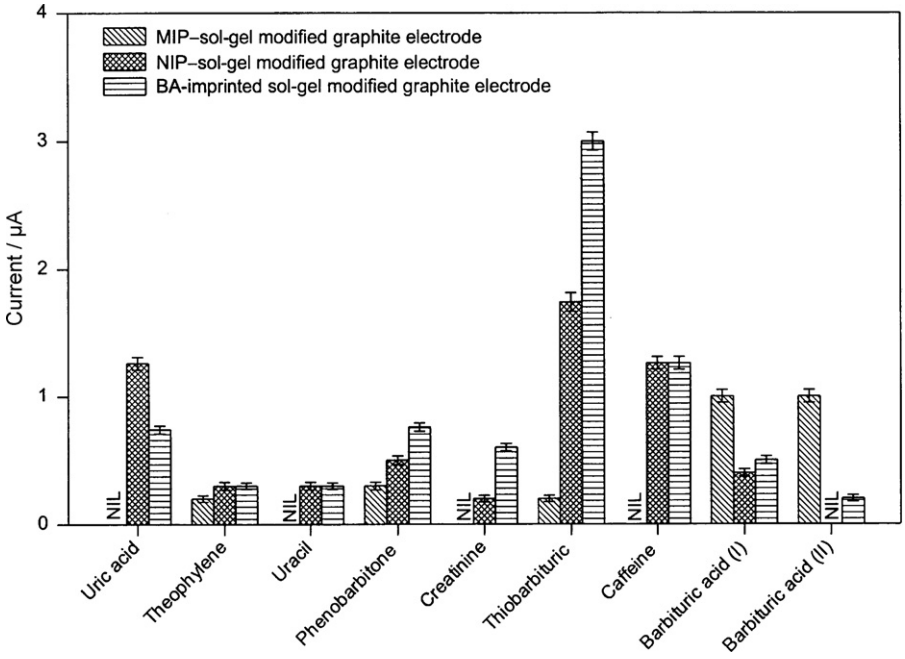

Fig. 4. Sensor response for BA (concentration 28.30 $\mu g\,mL^{-1}$) [(I) without water washing and (II) with water washing (1×5 mL)] and interferents (concentration 28.30 $\mu g\,mL^{-1}$) studied individually in aqueous solutions. Other conditions as in Fig. 3.

Table 2
Analytical results of DPCSV measurements of BA in the presence of interferents at MIP – sol–gel-modified graphite electrode.

Sample	Analyte BA concentration ($\mu g\,mL^{-1}$)	Determined value[a] (mean ± SD) ($\mu g\,mL^{-1}$) with MIP – sol–gel-modified graphite electrode	Recovery[b] (%)	Relative standard deviation (%) ($n = 3$)
Interferents[c]	41.66 (41.66 UA)	40.54 ± 0.82	97.3	2.0
	30.00 (300.00 UA)	29.70 ± 0.70	99.0	2.3
	30.00 (300.00 Tph)	30.09 ± 1.42	100.3	4.7
	30.00 (300.00 Ura)	30.00 ± 0.72	100.0	2.4
	26.78 (26.78 phBA)	26.30 ± 1.50	98.2	5.7
	26.78 (26.78 Cre)	26.88 ± 2.15	100.4	8.0
	30.00 (300.00 Cre)	30.00 ± 0.97	100.0	3.2
	26.78 (26.78 TBA)	28.23 ± 0.30	105.4	1.0
	30.00 (300.00 TBA)	29.59 ± 0.31	98.6	1.0
	26.78 (26.78 Caff)	26.80 ± 0.79	100.0	2.9
	30.00 (300.00 Caff)	29.59 ± 1.52	98.6	5.1
	10.00 (50.00 mix)[d]	10.43 ± 0.73	104.3	7.0
	83.33 (50.00 mix)[d]	82.80 ± 0.50	99.3	0.6

[a] Average value of three determinations ($S/N = 3$) with MIP–sol–gel-modified electrode.
[b] Amount of analyte determined/amount of analyte taken.
[c] Values in parentheses indicate concentration ($\mu g\,mL^{-1}$) of various interferents taken with BA in aqueous mixture solution. Interferents: Uric acid (UA); Theophylene (Tph); Uracil (Ura); Phenobarbitone (phBA); creatinine (Cre); thiobarbituric acid (TBA); Caffein (Caff).
[d] Mix denotes mixtures of UA, Tph, Ura, phBA, Cre, TBA, Caff (concentration 50.00 $\mu g\,mL^{-1}$ each).

3.5. Cross reactivity studies

Modified graphite electrodes prepared with MIP–sol–gel, NIP–sol–gel, and imprinted sol–gel, were subjected to cross-reactivity with different interferents, viz., uric acid, thiophylene, uracil, phenobarbitone, creatinine, thiobarbituric acid, caffein. As revealed from Fig. 4, MIP-modified sol–gel electrode (without washing treatment) is not responsive for all the interferents (except phenobarbitone, thiobarbituric acid and thiophylene) when studied individually. As far as BA detection is concerned with this electrode, it appeared highly specific, quantitative and unaltered after water-washings (c.f. BA (I) and BA (II), Fig. 4). The highest non-specific sorption with NIP-modified electrode was found for thiobarbituric acid and lowest for creatinine; though these non-specific sorptions for all interferents were easily mitigated from MIP-modified sol–gel surface simply by water-washing. The sol–gel-modified electrode did not yield quantitative response of BA, however this was responsive to the some extent to all interferents.

A parallel cross-reactivity study in the presence of BA (core) is necessary since real samples are always prevalent with concomitant interferents. The corresponding results are portrayed in Table 2. It is interesting to note that the proposed sensor, even without water washings after analyte recapture, revealed quantitative sorption of BA in binary and multiple mixtures (Table 2, Fig. 3f). This could be attributed to the film morphology as polymer brush which only allowed specific binding of BA in its hydrophobic domain of binding sites while pushing interferents away beyond brush tips in hydrophilic domain in aqueous environment. Thus any question of false-positive results owing to non-specific contributions is ruled out in the present investigation.

4. Conclusions

In this paper, a cost-effective, robust, renewable, disposable, and highly reproducible MIP-brush sensor invoking sol–gel technology in "grafting-to" approach is proposed for trace-level analysis of BA in real samples. The detection limits were found to be as low as 1.6 $\mu g\,mL^{-1}$ in aqueous, 1.8 $\mu g\,mL^{-1}$ in blood plasma, and 3.4 $\mu g\,mL^{-1}$ in human urine samples. These sensitivity limits are apparently enough to confirm long-acting possible cases of barbiturate poisonings (fatal dose >2 $\mu g\,mL^{-1}$ in 100-fold diluted blood plasma clinically, without any sample pretreatment and cross-reactivity. The performance of MIP used in the present study is being further improved in our laboratory by interfacing the proposed sensor with a suitable solid-phase micro extraction system in order to monitor intermediate and short-acting barbiturates in clinical samples. Nevertheless, in contrast to the major limitation of MIP usually occurred from slow mass-transfer, the MIP–film coating in the proposed IPN between graphite and sol–gel and in between sol–gel and exterior MIP brush interface actually augmented the mass-transfer kinetics and thereby response time of 90 s to yield quantitative results, without any false-positive (non-specific) contributions. The proposed MIP–sol–gel-modified graphite electrode is better than MIP-modified HMDE sensor (Prasad and Lakshmi, 2005) in terms of its practical utility for in-field clinical investigations, without any environmental hazards.

Acknowledgements

The support of this work by the Department of Science and Technology, New Delhi through the project SR/SI/IC-18/2006 is gratefully acknowledged.

References

Aboul-Enein, H.Y., Baeyens, W., Oda, H., Van Overbeke, A., 1996. Direct enantiomeric HPLC separation of several 2-arylpropionic acids, barbituric acids and benzodiazepines on chiracel OJ-R chiral stationary phase. Chromatographia 43, 599–606.
Advincula, R.C., Brittain, W.J., Caster, K.C., Rühe, J., 2004. Polymer Brushes: Synthesis, Characterization, Application. Wiley-VCH, Weinheim.
Aman, T., Khan, I.U., Parveen, Z., 1997. Spectrophotometric determination of barbituric acid. Anal. Lett. 30, 2765–2777.
Auroy, P., Auvray, L., Leger, L., 1991. Building of a grafted layer. 1. Role of the concentration of free polymers in the reaction bath. Macromolecules 24, 5158–5166.
Bailey, D.N., Jatlow, P.I., 1975. Barbital overdose and abuse. Am. J. Clin. Pathol. 64, 291–296.
Bartzatt, R., 2002. Determination of barbituric acid, utilizing a rapid and simple colorimetric assay. J. Pharm. Biomed. Anal. 29, 909–915.
Blanke, R.B., 1986. Analysis of toxic substances. In: Tietz, N.W. (Ed.), Clin. Chem., WB Saunders, New York, pp. 1670–1744.
Casoli, A., Brendle, M., Schultz, J., Auroy, P., Reiter, G., 2001. Friction induced by grafted polymeric chains. Langmuir 17, 388–398.
De Gennes, P.G., 1980. Conformation of polymer attached to an interface. Macromolecules 13, 1069–1075.
Dyer, D.J., 2003. Patterning of gold substrate by surface-initiated polymerization. Adv. Funct. Mater. 13, 667–670.
Garcia-Borregon, P.F., Lores, M., Cela, R., 2000. Analysis of barbiturates by micro-high-performance liquid chromatography with post-column photochemical derivatization. J. Chromatogr. 870, 39–44.
Julthongpiput, D., Lin, H.-Y., Teng, J., Zubarev, E.R., Tsukruk, V.V., 2003. Y-shaped amphiphilic brushes with suitable micellar surface. J. Am. Chem. Soc. 125, 15912–15921.
Kaaret, T.W., Evans, D.H., 1988. Voltammetry without supporting electrolyte using a platinum working electrode supported on an ion exchange membrane. Anal. Chem. 60, 657–662.

Lakshmi, D., Prasad, B.B., Sharma, P.S., 2006. Creatinine sensor based on a molecularly imprinted polymer-modified hanging mercury drop electrode. Talanta 70, 272–280.

Love, J.C., Wolfe, D.B., Chabinyc, M.L., Paul, K.E., Whitesides, G.M., 2002. Self-assembled monolayers of alkanethiolates on palladium are good etch resists. J. Am. Chem. Soc. 124, 1576–1577.

Luzinov, I., Julthongpiput, D., Malz, H., Pionteck, J., Tsukruk, V.V., 2000. Polystyrene layers grafted to epoxy-modified silicon surfaces. Macromolecules 33, 1043–1048.

Marzolin, C., Auroy, P., Deruelle, M., Folkers, J.P., Leger, L., Menelle, A., 2001. Neutron reflectometry study of the segment-density profile in end-grafted and irreversibly adsorbed layers of polymer in good solvents. Macromolecules 34, 8694–8700.

Medien, H.A.A., 1996. New method for spectrophotometric determination of quinines and barbituric acid through their reaction. A kinetic study. Spectro. Acta, Part A 52, 1679–1684.

Medien, H.A.A., Zahran, A.A., 2001. Spetrophotometric kinetic determination of quinine and barbiturates. Spectro. Acta, Part A 57, 2505–2511.

Nagaraja, P., Vasantha, R.A., Sunitha, K.R., 2001. A new sensitive and selective spectrophotometric method for the determination of catechol derivatives and its pharmaceutical preparations. J. Pharm. Biomed. Anal. 25, 417–424.

Nematollahi, D., Hesari, M., 2001. Electrochemical study of iodide in the presence of barbituric acid. Application to coulombic titration of barbituric acid. Microchem. J. 70, 7–11.

Netz, R.R., Schick, M., 1998. Polymer brushes: from self-consistent field theory to classical theory. Macromolecules 31, 5105–5122.

Patel, A.K., Sharma, P.S., Prasad, B.B., 2008. Development of creatinine sensor based on a molecularly imprinted polymer-modified sol-gel film on graphite electrode. Electroanalysis 20, 2102–2112.

Pawelczyk, E., Marciniec, B., Pluta, I., 1972. Application of infra-red spectrometry to quantitative assay of drugs. I. Infra-red spectrometry determination of some barbituric acid derivatives. Acta Pol. Pharm. 29, 382–390.

Podbielska, H., Ulatowska-Jarza, A., 2005. Sol-gel technology for biomedical engineering. Bull. Pol. Acade. Sci. Tech. Sci. 53, 261–271.

Prasad, B.B., Lakshmi, D., 2005. Barbituric acid sensor based on molecularly imprinted polymer modified hanging mercury drop electrode. Electroanalysis 17, 1260–1268.

Pyun, J., Matyajaszewski, K., 2001. Synthesis of nanocomposite organic/inorganic hybrid material using controlled/"living" radical polymerization. Chem. Mater. 13, 3436–3448.

Romer, M., Donaruma, L.G., Zuman, P., 1977. Spectrophotometric and polarographic analysis for phenobarbital, n-methylphenobarbital and n-methoxyphenobarbital in a mixture. Anal. Chim. Acta 88, 261–273.

Skoog, D.A., Holler, F.T., Nieman, T.A., 1998. Principles of Instrumental Analysis, 5th ed. Harcourt Brace College Publications, Philadelphia, p. 13.

Ubbink, J.B., Lagendiijk, J., Vermaak, W.H., 1993. Simple high-performance liquid chromatography method to verify the direct barbituric acid assay for urinary cotinine. J. Chromatogr. 620, 254–259.

Van Langenhov, A., Biller, J.E., Biemann, K., Browne, T.R., 1982. Simultaneous determination of phenobarbital and P-hydroxyphenobarbital and their stable isotope labeled analogs by gas chromatography and mass spectrometry. Biomed. Mass Spectrom. 9, 201–207.

Walsh, R., Becerra, R., 1998. Chemistry of Organic Silicon Compounds, In: Apeloig, Z. (Ed.), Rappoport. Wiley, Chichester, United Kingdom 2, p. 153.

Walters, K.B., Hirt, D.E., 2007. Synthesis and characterization of a tertiary amine polymer series from surface-grafted poly (tert-butyl acrylate) via diamine reactions. Macromolecules 40, 4829–4838.

Xu, J., Yang, C.S., Choi, C.K., 2004. Annealing effect on the structural and electrical properties of SiOC(-H) film with low dielectric constant prepared by plasma-enhanced chemical vapor deposition. J. Korean Phys. Soc. 45, 175–179.

You, T., Yang, X., Wang, E., 2000. Determination of barbituric acid and 2-thiobarbituric acid with end-column electrochemical detection by capillary electrophoresis. Talanta 51, 1213–1218.

Zdyrko, B., Swaminatha, K.I., Luzinov, I., 2006. Macromolecular anchoring layers for polymer grafting: comparative study. Polymer 47, 272–279.

Zhang, Z., Nie, L., Yao, S., 2006. Electrodeposited sol-gel-imprinted sensing film for cytidine recognition on Au-electrode surface. Talanta 69, 435–442.

Zhulina, E.B., Borisov, O.V., Priamitsyn, V.A., 1990. Theory of steric stabilization of colloid dispersions by grafted polymers. J. Colloid Interface Sci. 137, 495–511.